# Evidence for humid conditions during the last glacial from leaf wax patterns in the loess-paleosol sequence El Paraíso, Central Spain

Imke K. Schäfer[a,*], Marcel Bliedtner[a], Daniel Wolf[b], Dominik Faust[b], Roland Zech[a]

[a] *Institute of Geography and Oeschger Centre for Climate Change Research, University of Bern, Hallerstrasse 12, CH-3012 Bern, Switzerland*

[b] *Department of Geography, Technical University of Dresden, Helmholtzstraße 10, DE-01069 Dresden, Germany*

[*] Corresponding author: imke.schaefer@giub.unibe.ch (I.K. Schäfer).

## Abstract

The Mediterranean region is affected by the first consequences of anthropogenic climate change and suffers from aridization and drought periods. Reconstructing past climate and environmental changes might help to put those consequences into context, identify underlying mechanisms and improve predictions. Here we present leaf wax analyses for the loess-paleosol sequence (LPS) from El Paraíso, located in Central Spain and a selection of plants growing there today. The long-chain *n*-alkanes in almost the whole LPS are characterized by the dominance of $C_{29}$, $C_{31}$ and $C_{33}$, indicating the presence of grasses and drought-adapted tree species, such as *Juniperus* and *Olea*. However, samples correlated with marine isotope stage (MIS) 2 (~29 to 14 ka) have higher abundances of $C_{25}$, $C_{27}$ and $C_{29}$, which may signal the presence of less drought-adapted deciduous trees and more humid conditions. *n*-

Alkanoic acid patterns can tentatively be interpreted to confirm these results, but are less robust, because more plant species are needed for comparison. Our findings and interpretation are in line with climate modelling studies that suggest a southward shift of the westerlies and storm tracks during MIS 2, with fluvial and lacustrine records, and with glacial refugia for temperate trees in southern Europe. Compound-specific isotope analyses will hopefully soon provide additional information about paleoclimatic and –hydrologic changes and help establish a more precise and robust age control.


## Keywords

Climate reconstruction; leaf wax biomarkers; *n*-alkanes; *n*-alkanoic acids; Loess-paleosol sequences; Iberia


## 1. Introduction

Today's climate change is of great importance. Hardly a day goes by without reports about extreme weather phenomena like hurricanes, droughts and floods in some regions of the earth. To better understand the mechanisms and environmental consequences of recent anthropogenic climate change, it is indispensable to reconstruct past climate and environmental changes, especially in regions that already suffer today. More and more attention is being paid, for example, to the Mediterranean region, which is prone to droughts and affected by aridization (Giorgi and Lionello, 2008; Seager et al., 2014). Paleoclimatically, the Iberian Peninsula is a

very interesting location, because its climate is influenced by the polar front, the storm tracks from the North Atlantic, the Mediterranean Sea, and by its proximity to Africa and Africa's monsoons (Bout-Roumazeilles et al., 2007; Lewis et al., 2009; Beghin et al., 2015).

Information from Iberia about past climate and environmental changes is sparse and contended. One controversy arose from findings that glaciers in some parts of Iberia may have already reached the maximum extent before the global Last Glacial Maximum (LGM: ~25 to 19 ka, Clark et al. 2009; e.g. Pallàs et al., 2006 and references therein; Lewis et al., 2009). Another long-standing controversy concerns the hydrological conditions during the LGM. Pollen records are traditionally interpreted as indicating more arid conditions, whereas lacustrine and fluvial records, as well as climate models, all suggest more precipitation (Prentice et al., 1992; recent reviews of Moreno et al., 2012; Moreno et al., 2014; Beghin et al., 2015 and references therein).

Increasingly, new and interesting insights may soon come from biomarker analysis in LPS. Compared to pollen records, which are mostly established from lake sediments and peat bogs (i.e. from specific topographical and microclimatological settings), biomarker records can provide valuable complementary paleoenvironmental information. This is because LPS occur on plateaus and in protected slope positions. Although pollen is often not preserved in LPS, some biomarkers are (Zhang et al., 2006; Zech et al., 2011). Loess is often interpreted as

documenting glacial, cold and arid conditions, and paleosols as documenting more humid conditions during interglacials and interstadials (Garcia Giménez et al., 2012; Zech et al., 2013). However, variable dust accumulation rates need to be taken into account, which is why proxies independent of dust accumulation rate, such as biomarkers, are particularly valuable.

Long chain *n*-alkanes and *n*-alkanoic acids are essential constituents of epicuticula leaf waxes that are produced by all types of plants to protect them from water stress and microbial attack (Eglinton and Hamilton, 1967; Gülz, 1994; Eglinton and Eglinton, 2008). Because of this protective function, leaf waxes can be highly inert; hence, they can be preserved in soils and sediments over geological timescales and serve as biomarkers. Numerous studies have investigated the chemotaxonomic potential of leaf waxes (Cranwell, 1973; Ficken et al., 1998; Maffei et al., 2004; Rommerskirchen et al., 2006; Zech et al., 2009; Zocatelli et al., 2012). Higher abundances of the *n*-$C_{27}$ and *n*-$C_{29}$ alkanes have been found to be characteristic for deciduous trees and shrubs, while the longer alkane homologues *n*-$C_{31}$ and *n*-$C_{33}$ are more abundant in grasses and herbs. We recently conducted a transect study in Central Europe and were able to confirm this pattern (Schäfer et al., submitted). Moreover, we found the *n*-$C_{24}$ alkanoic acid to be particularly abundant under coniferous trees, the *n*-$C_{28}$ alkanoic acid under deciduous trees, and grasslands to have relatively high amounts of *n*-$C_{32}$ and *n*-$C_{34}$ (Schäfer et al. submitted). Leaf wax production and homologue patterns can be highly variable, even within plants belonging to the same vegetation type (Diefendorf et al., 2011; Bush and McInerney,

2013; Schäfer et al., submitted). Therefore, vegetation reconstructions (i) should be evaluated against leaf wax patterns at a regional scale, and (ii) might be biased or even flawed due to specific species. Climate conditions, such as changes in temperature, precipitation and relative humidity, may influence the homologue patterns (e.g. Poynter, 1989; Sachse et al., 2006; Tipple and Pagani, 2013; Bush and McInerney, 2015). Nevertheless, leaf waxes have been successfully applied in many paleostudies (e.g. Brincat et al., 2000; Schwark et al., 2002; Zhang et al., 2006; Zech et al., 2010; Tarasov et al., 2013).

For this study we analysed *n*-alkanes and *n*-alkanoic acids in the LPS El Paraíso, as well as in some plants growing at and near that site. The objectives of our study were (i) to test whether or not leaf wax patterns of local common plants are in line with homologue patterns typical for vegetation types in Central Europe; and (ii) to use the leaf wax patterns in the LPS El Paraíso to infer changes in paleoenvironmental conditions during the Late Quaternary in Central Spain.

## 2. Regional setting, climate and vegetation

### 2.1 Regional setting

The LPS El Paraíso (560 m a.s.l., N 40° 01.855‘ W 03° 28.031‘) is located east of Aranjuez (Fig 1a) on north facing slopes that mediate between the Mesa de Ocaña and the incised river valley s of the Tagus River. The Tagus is the longest river of the Iberian Peninsula and it has the third largest catchment area (Benito et al., 2003). The Tagus Basin evolved during the Tertiary with thick successions of

114 alluvial fan material and lacustrine deposits (Calvo et al. 1996). These sediments
115 consist of evaporites that are assigned to the Miocene Lower Unit and the Miocene
116 Intermediate Unit. The sediments of the Miocene Upper Unit are transformed into
117 conglomerates and lacustrine limestones (Garcia Giménez et al., 2012 and references
118 therein). After intense dissection of these basin deposits, Pleistocene and Holocene
119 deposits have accumulated above the Miocene marls (Roquero et al., 2015; Wolf and
120 Faust 2015). Today, these Quaternary sediments are mainly exposed along the valley
121 floor and the remains of river terraces where also the main loess outcrops occur (Fig. 1b;
122 Garcia Giménez et al., 2012).

123 **2.2 Climate and vegetation**

124 Today's climate in Central Spain is Mediterranean, with warm arid summers and
125 more humid mild winters. While the summer regime is controlled by the subtropical
126 anticyclone of the Azores, the conditions during winter are strongly affected by the
127 westerlies (Benito et al., 2003, Beghin et al., 2015). Most of the annual precipitation
128 occurs during winter when cold air masses from the North Atlantic are mixed with
129 warmer and more humid ones leading to precipitation. Annual rainfalls are
130 moderate (400-500 mm, García et al., 2011), and mean annual temperatures are
131 between 11-14°C (Roquero et al., 2015).

132

133 The modern vegetation has adapted to these particular conditions. Large parts of
134 the region are inhabited by *Quercus ilex*. Other typical tree species in this region are
135 *Pinus nigra*, *Quercus lusitanica*, *Juniperus sabina*, *Pinus maritime* and *Olea*
136 *europaea*. The lower plant layers are composed of *Juniperus* and *Quercus* species,

137 *Thymus vulgaris*, *Asparagus acutifolius*, *Salvia lavandulaefolia* and *Rosmarinus*
138 *officinalis*. Xerophytic and halophytic grasses, and herbs like *Stipa tenacissima*,
139 build up the herb layer. However, the potential natural vegetation has been strongly
140 reduced due to human intervention, thus the modern vegetation cover surrounding the
141 LPS El Paraíso mainly consists of almond trees (*Prunus dulcis*) and grass species, e.g.
142 *Stipa tenacissima* and *Cupressus sempervirens*.
143

144 # 3. Material and Methods

145 ## 3.1 Sampling and sample material

146 The LPS El Paraíso is 8 m high and consists of alternating units of reddish ochre
147 loess and fossil soils (Fig. 1c). The upper part (<4 m depth) is characterised by low
148 conductivity (<800 $\mu Scm^{-1}$) and the absence of calcareous concretions. Intercalated
149 soil horizons show various but mainly low degrees of weathering. The sediments of
150 the lower part (>4 m depth) consist of partly reworked material. They are
151 characterised by an increase in clay content (>15%) and calcareous concretions of
152 various sizes. Here, soil horizons appear much stronger developed indicating more
153 intense weathering processes. A detailed sedimentological and pedological
154 description is provided by Wolf et al. (in preparation). They investigated several LPS
155 along the Tagus River. Magnetic susceptibility and further parameters made it
156 possible to correlate the sequences and revealed ages of ~25 ka and ~35 ka for the
157 paleosols at ~2 and ~4.5 m depth in the LPS El Paraíso, dates which were based on
158 luminescence ages in the LPS Fuentidueña (not shown). Preliminary luminescence

159 ages from the LPS El Paraíso suggest that the paleosol at ~2 m depth might actually
160 be slightly older, and first compound-specific $^{14}C$ analyses identify the soil at ~1 to
161 1.4 m depth as Holocene soil and the overlying sediments as colluvium. The loess
162 sediments from ~1.0 to 1.9 m depth were thus most likely deposited during MIS 2
163 and overprinted in the upper part by Holocene pedogenesis.
164
165 Soil and sediment samples were taken during a field trip in March 2014. At least
166 one sample per paleosol/loess horizon was taken, and 31 samples in all were
167 available for biomarker analyses. The samples were dried immediately after
168 sampling. In September 2014, ten vegetation samples were collected from living
169 plants, which are common in the study area. The samples are comprised of leaves
170 from broadleaf evergreen *Quercus coccifera*, *Quercus ilex* and *Olea europea*, as well
171 as needles from *Juniperus phoenicea*, *Juniperus thurifera*, *Pinus halepensis* and
172 *Pinus nigra*. In addition, a herbaceous plant (*Thymus vulgaris*) and a
173 Mediterranean grass species (*Stipa tenacissima*) were sampled. These samples were
174 also dried immediately after sampling.

175 **3.2 Biomarker analyses**

176 1 g fresh plant material was extracted by using microwave assisted solvent
177 extraction with 15 ml dichloromethane (DCM)/methanol (MeOH) (9:1) at 100°C for 1
178 h. For the paleosols, ~40 g sediment were extracted with an Accelerating Solvent
179 Extractor (Dionex 200, two extraction cycles, 6.9 MPa, 100°C), and by using the
180 same solvent mixture as for the plant samples. Total lipid extracts were passed over
181 pipette columns filled with aminopropyl silica gel (Supelco, 45 μm). The aliphatic

fraction (incl. *n*-alkanes) was eluted with hexane, more polar compounds (e.g. alcohols) with DCM/MeOH (1:1), and acids (incl. *n*-alkanoic acids) with 5% acetic acid in diethylether. The *n*-alkanoic acids were converted to fatty acid methyl esters (FAMEs) by using MeOH/HCl (95/5; 70°C, overnight). The FAMEs were recovered by using liquid-liquid extraction with hexane. The aliphatic fraction and the acid fraction were spiked with a known amount of an internal standard (5α-androstanone) and analyzed by gas chromatography-mass spectrometry (GC-MS). The analysis was carried out by using an Agilent MS 5975 (EI) interfaced with an Agilent 7890 GC equipped with a 30 m fused silica capillary column (HP5-MS 0.25 mm i.d., 0.25 µm film thickness), and a split/splitless injector operating in splitless mode at 350°C. Carrier gas was helium and the temperature program was 1 min at 50°C, from 50 to 200°C at 30°C$min^{-1}$, from 200 to 320°C at 7°C$min^{-1}$, 5 min at 320°C. Data recording comprised the Total Ion Current (TIC, scan mode from m/z 40 to m/z 600) and SIM (Single Ion monitoring) scan (m/z 57, 71, 85 and 99). Concentrations were calculated relative to the internal standard and to an external standard (*n*-$C_{20}$ to *n*-$C_{40}$ alkane mixture, Supelco), injected in different concentrations (40 ng/µl, 4 ng/µl, 1 ng/µl, 0.4 ng/µl).

### 3.3 Data analyses

Total *n*-alkane and *n*-alkanoic acid concentrations ($c_{tot}$) are calculated as the sums of $C_{25}$ to $C_{35}$ and $C_{20}$ to $C_{34}$, respectively. The average chain length (ACL) describes variations in chain lengths of *n*-alkanes (Poynter et al., 1989).

ACL (*n*-alkanes) = (27 x $n$-$C_{27}$ + 29 x $n$-$C_{29}$ + 31 x $n$-$C_{31}$ + 33 x $n$-$C_{33}$)/($n$-$C_{27}$ + $n$-$C_{29}$ + $n$-$C_{31}$ + $n$-$C_{33}$) (1)

The odd/even predominance (OEP) of the *n*-alkanes and the even/odd predominance (EOP) of the *n*-alkanoic acids was determined following Hoefs et al. (2002):

OEP = ($n$-$C_{27}$ + $n$-$C_{29}$ + $n$-$C_{31}$ + $n$-$C_{33}$)/($n$-$C_{26}$ + $n$-$C_{28}$ + $n$-$C_{30}$ + $n$-$C_{32}$) (2)

EOP = ($n$-$C_{24}$ + $n$-$C_{26}$ + $n$-$C_{28}$ + $n$-$C_{30}$ + $n$-$C_{32}$)/($n$-$C_{23}$ + $n$-$C_{25}$ + $n$-$C_{27}$ + $n$-$C_{29}$ + $n$-$C_{31}$) (3)

The *n*-alkanoic acid indices C, D and G were calculated according to Schäfer et al. (submitted). These indices show the input of conifers (C), deciduous trees (D) and grasses (G) respectively:

Index C = ($n$-$C_{24}$)/( $n$-$C_{24}$ + $n$-$C_{28}$ + $n$-$C_{32}$ + $n$-$C_{34}$)

Index D = ($n$-$C_{28}$)/( $n$-$C_{24}$ + $n$-$C_{28}$ + $n$-$C_{32}$ + $n$-$C_{34}$)

Index G = ($n$-$C_{32}$ + $n$-$C_{34}$)/( $n$-$C_{24}$ + $n$-$C_{28}$ + $n$-$C_{32}$ + $n$-$C_{34}$)

# 4. Results and Discussion

## 4.1 *n*-Alkane patterns in plants

$C_{tot}$ in the sampled plants range from 3.9 µg/g to 391 µg/g dry weight (Tab. 1). *Pinus h.* and *Pinus n.* have very low *n*-alkane concentrations, which is typical for conifers (e.g. Diefendorf et al., 2011; Zech et al., 2012; Bush and McInerney, 2013). However, *Juniperus p.* and *Juniperus t.* have high concentrations. This is unusual for conifers, but has been reported previously (Tarasov et al., 2013). While the needles of the two *Juniperus* species and *Pinus n.* are dominated by the *n*-$C_{33}$ alkane, the needles of *Pinus h.* show a dominance of the $C_{29}$ and $C_{31}$ *n*-alkanes, although not a pronounced. $C_{tot}$ in *Quercus c.* and *Quercus i.* is high (Tab. 1). Both those species show a strong dominance of the *n*-$C_{29}$ alkane, which is consistent with previous studies on leaves in Italy (Sachse et al., 2006) and on leaves and soils below *Quercus* in Central Spain (Almendros et al., 1996). *Olea e.* also has a high $c_{tot}$, but shows a dominance of the *n*-$C_{33}$ alkane, which is normally regarded as a marker for grasses and herbs. Since *Olea e.* is a species adapted to pronounced variations in temperature and precipitation (Pantaléon-Cano et al., 2003), the preferential synthesis of longer chain leaf waxes might be a distinct protective mechanism compared to other deciduous trees. Other studies have found a dominance of *n*-$C_{31}$ in *Olea* (Bianchi et al., 1992; Mihailova et al., 2015). Also, Bianchi et al. (1992) showed that *Oleas* leaf wax production was quite unique in the sense that it produces pentacyclic triterpenes as dominant leaf wax group. The samples of *Thymus v.* and S*tipa t.* have high *n*-alkane concentrations. Both species show a dominance of long chains (*n*-$C_{33}$: *Thymus v.* and *n*-$C_{31}$: *Stipa t.*), which is typical for grasses and herbs.

In summary, these results suggest that *n*-alkanes may be useful biomarkers to infer past environmental conditions. Shorter chains ($C_{27}$ and $C_{29}$) may indicate the presence of deciduous trees, as well as *Quercus i.* and *c.*, whereas longer chains ($C_{31}$ and $C_{33}$) may indicate the presence of grasses and herbs, as well as trees, such as *Olea* and *Juniperus*, which are particularly well adapted to arid conditions. Conifers other than *Juniperus* are probably not represented in the sedimentary archives.

As *n*-alkane homologue patterns have been shown to be affected by degradation, Zech et al. (2009) proposed an endmember model for corrections. Endmember plots use a normalized *n*-alkane ratio on the y-axis, and the OEP as a proxy for degradation (e.g. Tipple and Pagani, 2010; Vogts et al., 2012; Wang et al., 2014) on the x-axis. In general, *n*-alkane ratios are wider for grasses and soils from grasslands, and narrower for samples from deciduous trees and respective soils. However, with increasing degradation (lower OEPs), differences become less, illustrated and quantitatively described by "degradation lines" (Fig. 2a). In principal, the endmember model can be used to quantify the leaf wax contributions from deciduous trees and grasses, but one should keep in mind the wide variability of the homologue patterns.

Due to the relatively high amounts of *n*-alkanes $C_{31}$ and $C_{33}$, *Olea e.* plots far above the degradation line for deciduous trees from Central Europe, and it even plots above the degradation line for grasslands (Fig. 2a). Both *Quercus* species likewise plot above the degradation line for deciduous trees. As mentioned above, this likely

reflects an adaptation to arid and warm conditions in Central Spain. *Stipa t.* and *Thymus v.* plot close to the degradation line for grasslands. The *Juniperus* samples also plot close to the grassland degradation line. We chose not to plot the *Pinus* samples, due to their low *n*-alkane concentration, which makes them irrelevant when interpreting sediment *n*-alkane patterns.

All in all, Fig. 2a illustrates that the endmember model for Central Europe can be used in Iberia to evaluate and correct degradation effects on *n*-alkane patterns in sedimentary archives. But it also shows that quantitative interpretations (in terms of deciduous trees vs. grass contributions) are likely biased by the adaptation of plants to arid and warm conditions. High reconstructed and modelled "grass percentages" can therefore be interpreted as signs of more arid conditions, but should not be regarded as exclusive concerning drought-adapted species, such as *Juniperus* and *Olea*. More plant samples from the Mediterranean region need to be studied to refine this picture, but we will nevertheless try to use *n*-alkanes and the endmember model in the LPS El Paraíso for paleoenvironmental reconstruction.

### 4.2 *n*-Alkane patterns in the LPS El Paraíso

$C_{tot}$ in the samples from the LPS El Paraíso range from 4.7 µg/g to 0.04 µg/g dry sediment (Fig. 3). Concentrations are higher in the upper part of the sequence yet decrease with depth, which is probably due to enhanced degradation in the deeper layers of the LPS. Interestingly, the pattern of the OEP does not follow this trend. Overall, OEP values >4 throughout the whole profile show good preservation (Zech

et al., 2009), but values are lowest in the MIS 2 loess (~1.4 to 1.9 m depth) and then increase again with depth. The *n*-alkanes that survived degradation in the lower part of the profile are possibly stabilized by a mechanism that prevents preferential degradation of odd vs. even chains, which is typically found during degradation of fresh plant material. ACL ranges from 30.6 to 29.3, and the lowest values are at ~1.4 to 1.9 m depth (Fig. 3). The *n*-alkane ratio ($n$-$C_{31}$+$n$-$C_{33}$)/($n$-$C_{27}$+$n$-$C_{31}$+$n$-$C_{33}$) strongly correlates with the ACL, and also has its lowest values in the MIS 2 loess sediments.

Before interpreting these chain-length patterns paleoecologically, we evaluated the degree to which they may have been biased by degradation effects. In the endmember plot (Fig. 2b), most samples fall close to the degradation line of grasses and only a few data points are closer to the degradation line of deciduous trees. Although we calculated "grass contribution %" for all samples from the endmember model, and plotted the respective values (Fig. 3), we explicitly emphasize that they are *not* to be interpreted in terms of leaf wax inputs from grasses. We say this, because *Juniperus* and *Olea* are characterized by longer chain lengths. Instead, the endmember calculations simply show that the homologue patterns in the LPS El Paraíso are not only an artefact of degradation. "Grass contribution %" closely correlates with the ACL and the *n*-alkane ratio. All three plots suggest that grasses and drought-adapted species, like *Juniperus* and *Olea*, were likely dominant at our research site during most of the Late Quaternary. Deciduous trees *less* adapted to drought seem to have been more prevalent only during MIS 2. Our results and

313 interpretation are in line with fluvial and lacustrine records from Iberia, which
314 suggest there were more humid conditions during the global LGM, probably due to a
315 southward shift of the westerlies and storm tracks (Moreno et al., 2012; Moreno et
316 al., 2014; Beghin et al., 2015). Our results and interpretation are also in line with
317 genetic features of recent European tree populations, which show that tree species
318 survived in glacial refugia in Southern Europe during the last glacial (Carrión et al.,
319 2003; González-Sampériz et al., 2010). At first glance, all these findings seem to
320 contradict pollen records, which indicate steppe vegetation during the last glacial
321 (Pantaléon-Cano et al., 2003; González-Sampériz et al., 2006; González-Sampériz et
322 al., 2010). Therefore future studies should investigate the complementary nature of
323 the various archives and proxies. Local, microclimatic and ecological differences and
324 variability have to be considered. Wolf and Faust (2015), for example, have shown
325 strong spatial heterogeneity of physiographic and climatic conditions on the Iberian
326 Peninsula for the Holocene epoch. Specific strengths, weaknesses and potential
327 pitfalls, e.g. pollen and leaf wax production during the last glacial, when $CO_2$
328 concentrations were lower and winds probably stronger, also have to be considered.
329 One obvious limitation of the *n*-alkane proxy is that it is nearly blind for conifers
330 (*Juniperus* is an exception). Since pines are believed to be an important component
331 of glacial forests in the Iberian Peninsula (Rodríguez-Sánchez et al., 2010), this
332 motivated us to also explore the potential of *n*-alkanoic acids as leaf wax biomarkers
333 for paleoenvironmental reconstructions.
334

### 4.3 *n*-Alkanoic acid patterns in plants

$C_{tot}$ of the long chain *n*-alkanoic acids ranges from 12.6 to 62.5 µg/g dry weight (Tab. 2). The maximum long chain *n*-alkanoic acid in the two *Juniperus* species is *n*-$C_{28}$ (Tab. 2), which is longer than in the study of Almendros et al. (1996), who found a dominance of *n*-$C_{22}$ and *n*-$C_{24}$ in soils below *Juniperus*. On the other hand, both *Pinus* species have a clear dominance of $C_{24}$, which is consistent with the previous study. The two *Quercus* species show maxima for *n*-$C_{28}$ and *n*-$C_{24}$., and Almendros et al. (1996) found a *n*-$C_{24}$ dominance in *Quercus*. In *Olea e.* we found a dominance of *n*-$C_{32}$, whereas Bianchi et al. (1992) reported *n*-$C_{28}$ to be predominant in leaves of *Olea* in Italy. *Thymus v.* has a dominance of *n*-$C_{24}$ and *Stipa t.* shows a high amount of *n*-$C_{28}$.

In the following section, we compare the *n*-alkanoic acid patterns with those from the transect study in Central Europe (Schäfer et al., submitted). There, we found $C_{24}$ acid to be particularly abundant in conifers, while *n*-$C_{28}$ appeared to be preferentially synthesized by deciduous trees, and grasslands showed relatively high amounts of *n*-$C_{32}$ and *n*-$C_{34}$. In a CDG ternary plot (Fig. 4a), samples accordingly plot in distinct clusters. Here, we marked only the position of the respective means for conifers, deciduous trees and grasses.

The two *Pinus* species from Central Spain have very high C indices and plot in the "correct" corner for coniferous trees. Our *Juniperus* samples, however, plot closer to the endmember of deciduous trees. As noted above, Almendros et al. (1996) found a

dominance of $C_{22}$ and $C_{24}$ in soils under *Juniperus*, so their samples would plot closer to the expected location based on comparison with the endmembers from Central Europe. Our *Olea* sample has a very high G index. Again, previously reported *n*-alkanoic acid patterns are different, as Bianchi et al. (1992) reported $C_{28}$ dominance for *Olea* from Italy. As for our *n*-alkanes, we suggest that *Juniperus* and *Olea* adapt to the arid and warm conditions in Central Spain by synthesizing longer *n*-alkanoic acids. *Quercus c.* has a very high D index, but to our surprise *Quercus i.* has a dominance of shorter homologues and a high C index. *Stipa t.* has a high D index and plots unexpectedly far from the grass endmember, whereas *Thymus v.* has a low D index and plots relatively close to the coniferous endmember. Overall, these findings illustrate the variability of the *n*-alkanoic acid homologue patterns. They also demonstrate the need to substantially enlarge the number of plant samples from Iberia and Southern Europe before the CDG indices can be robustly used in paleoenvironmental reconstructions.

### 4.4 *n*-Alkanoic acid patterns in the LPS El Paraíso

We evaluated the *n*-alkanoic acid variability in the LPS El Paraíso. $C_{tot}$ of *n*-alkanoic acids range from 9.5 μg/g in the uppermost sample to 0.01 μg/g dry sediment in the deepest one (Fig. 5). Concentrations drop dramatically below 3 m depth. Low leaf wax biomarker concentrations could reflect very arid climate conditions and low vegetation density, but we suspect that degradation is also very relevant. EOPs are extremely low (close to 1, apart from 2 samples) in the upper part of the sequence, which indicates poor preservation of *n*-alkanoic acids, and EOPs could not even be

calculated below 3 m depth, because not all necessary compounds were above the detection limit.

In general, preservation of lipids in soils depends on various chemical and environmental factors, particularly soil pH (e.g. Nierop and Verstraten, 2003). While *n*-alkane preservation is favoured by higher soil pH, *n*-alkanoic acids are better preserved in more acidic soils (Bull et al., 2000). The arid conditions in Central Spain and high soil pH might thus explain the poor preservation status of the *n*-alkanoic acids in the LPS El Paraíso, particularly below ~3 m depth, i.e. before ~30 ka. More arid conditions before ~30 ka are in accordance with the interpretation of sedimentary *n*-alkanes and the presence of carbonate concretions below ~4 m depth.

Despite the wide variability of the *n*-alkanoic acid indices C, D and G in our modern vegetation samples, we calculated and plotted these indices for the LPS El Paraíso. We did so in order to check for systematic patterns and changes in paleovegetation. The *n*-alkanoic acid concentrations are high enough to calculate the indices only in the upper part of the sequence. The sample PA55 (Fig. 5) has a high C indice and plot close to the coniferous endmember in the CDG ternary plot. This suggests that *Pinus* and *Quercus i.* may have contributed most to the sedimentary leaf waxes. For the MIS 2 samples between ~1.4 and 1.9 m depth, relatively high D indices coincide with lower G indices, whereas generally lower D indices and higher G indices characterize the sediments and soils before ~30 ka. In the CDG ternary plot, the "MIS 2" samples therefore plot lower than the "MIS 3" samples (Fig. 4b). Although

assigning specific sources and robustly reconstructing past changes in vegetation are not possible at this stage, we speculate that the MIS 2 samples contain more input from *Quercus i.* and *c.*, and possibly also from deciduous trees, whereas the longer chain lengths in the MIS 3 samples reflect adaptations to more arid conditions. Such an interpretation would be consistent with the *n*-alkanes and would lend support to the assumption of an arid MIS 3 in Spain as documented by Álvarez-Lao et al., 2015.

## 5. Conclusions

- The *n*-alkane homologue patterns in plants from Central Spain are generally consistent with earlier observations and confirm the hypothesis that broadleaf trees, particularly deciduous trees, produce shorter chains than grasses and herbs. However, plants in Central Spain seem to adapt to the arid and warm conditions by synthesizing relatively long chains, as evidenced for example by the $C_{33}$ dominance in *Olea* and *Juniperus*.
- *n*-Alkane patterns in the LPS El Paraíso are characterized by shorter chain lengths during MIS 2, which lends support to the hypothesis that climate conditions in the Mediterranean region were *not* particularly arid. In fact, our findings, climate modelling studies, fluvial and lacustrine records, as well as glacial refugia for temperate trees in Southern Europe, all suggest the conditions were more humid than previously suggested mainly based on palynology.

- The *n*-alkanoic acid patterns of the plants vary substantially and, like the *n*-alkane patterns, indicate that adaptation to arid and warm climate involves preferential synthesis of longer chains. Longer chains in the LPS El Paraíso can tentatively be interpreted as confirming more arid conditions before ~30 ka, whereas more humid conditions can again be tentatively inferred for the MIS 2.

Many more plant samples from Central Spain and from Southern Europe are needed to corroborate the proposed relationships between leaf wax patterns and climate. This is particularly the case for the *n*-alkanoic acids. In the future, we plan to carry out compound-specific δD and $\delta^{13}C$ analyses on the leaf waxes from the LPS El Paraíso in order to obtain supplementary paleoclimatic and -hydrologic information (Sachse et al., 2012; Zech et al., 2013). Compound-specific $^{14}C$ analyses shall also be carried out to establish a more precise and robust chronology (Häggi et al., 2014).

## Acknowledgements

We thank M. Suhr, S. Lutz, L. I. Schweri and L. Wüthrich for help in the laboratory. This project was funded by SNSF (PP00P2 150590).

# References


Almendros, G., Sanz, J., Velasco, F., 1996. Signatures of lipid assemblages in soils under continental Mediterranean forests. European Journal of Soil Science 47, 183-196.

Álvarez-Lao, D.J., Ruiz-Zapata, M.B., Gil-García, M.J., Ballesteros, D., Jiménez-Sánchez, M., 2015. Palaeoenvironmental research at Rexidora Cave: New evidence of cold and dry conditions in NW Iberia during MIS 3. Quaternary International 379, 35-46.

Beghin, P., Charbit, S., Kageyama, M., Combourieu-Nebout, N., Hatté, C., Dumas, C., Peterschmitt, J.Y., 2015. What drives LGM precipitation over the western Mediterranean? A study focused on the Iberian Peninsula and northern Morocco. Clim Dyn, 1-21.

Benito, G., Sopeña, A., Sánchez-Moya, Y., Machado, M.a.J., Pérez-González, A., 2003. Palaeoflood record of the Tagus River (Central Spain) during the Late Pleistocene and Holocene. Quaternary Science Reviews 22, 1737-1756.

Bianchi, G., Vlahov, G., Anglani, C., Murelli, C., 1992. Epicuticular wax of olive leaves. Phytochemistry 32, 49-52.

Bout-Roumazeilles, V., Combourieu Nebout, N., Peyron, O., Cortijo, E., Landais, A., Masson-Delmotte, V., 2007. Connection between South Mediterranean climate and North African atmospheric circulation during the last 50,000 yr BP North Atlantic cold events. Quaternary Science Reviews 26, 3197-3215.

Brincat, D., Yamada, K., Ishiwatari, R., Uemura, H., Naraoka, H., 2000. Molecular-isotopic stratigraphy of long-chain *n*-alkanes in Lake Baikal Holocene and glacial age sediments. Organic Geochemistry 31, 287-294.

Bull, I.D., Bergen, P.F.v., Nott, C.J., Poulton, P.R., Evershed, R.P., 2000. Organic geochemical studies of soils from the Rothamsted classical experiments—V. The fate of lipids in different long-term experiments. Organic Geochemistry 31, 389-408.

Bush, R.T., McInerney, F.A., 2013. Leaf wax n-alkane distributions in and across modern plants: Implications for paleoecology and chemotaxonomy. Geochimica et Cosmochimica Acta 117, 161-179.

Bush, R.T., McInerney, F.A., 2015. Influence of temperature and $C_4$ abundance on *n*-alkane chain length distributions across the central USA. Organic Geochemistry 79, 65-73.

Calvo, J.P., Alonso-Zarza, A.M., Garcia del Cura, M.A., Ordoñez, S., Rodriguez-Aranda, J.P., Sanz Montero, M.E., 1996. Sedimentary evolution of lake systems through the Miocene of the Madrid Basin: paleoclimatic and paleohydrological constraints, In: Friend, P. F. and Dabrio, C. J. (ed.): Tertiary basins of Spain: the stratigraphic record of crustal kinematics, pp. 272–277.

Carrión, J.S., Yll, E.I., Walker, M.J., Legaz, A.J., Chaín, C., López, A., 2003. Glacial refugia of temperate, Mediterranean and Ibero-North African flora in south-eastern Spain: new evidence from cave pollen at two Neanderthal man sites. Global Ecology and Biogeography 12, 119-129.

Clark , P. U., Dyke, A. S., Shakun, J. D., Carlson, A. E., Clark, J., Wohlfarth, B., Mitrovic, J. X., Hostetler, S. W., Marshall McCabe, A. 2009. The Last Glacial Maximum. Science 325, 710-714.

Cranwell, P.A., 1973. Chain-length distribution of *n*-alkanes from lake sediments in relation to post-glacial environmental change. Freshwater Biology 3, 259-265.

Diefendorf, A.F., Freeman, K.H., Wing, S.L., Graham, H.V., 2011. Production of *n*-alkyl lipids in living plants and implications for the geologic past. Geochimica et Cosmochimica Acta 75, 7472-7485.

Eglinton, G., Hamilton, R.J., 1967. Leaf epicuticular waxes. Science 156, 1322-1335.

Eglinton, T.I., Eglinton, G., 2008. Molecular proxies for paleoclimatology. Earth and Planetary Science Letters 275, 1-16.

Ficken, K.J., Barber, K.E., Eglinton, G., 1998. Lipid biomarker, $\delta^{13}C$ and plant macrofossil stratigraphy of a Scottish montane peat bog over the last two millennia. Organic Geochemistry 28, 217-237.

Garcia Giménez, R., Vigil de la Villa, R., González Martín, J.A., 2012. Characterization of loess in central Spain: a microstructural study. Environmental Earth Science 65, 2125-2137.

Garcìa, R., Petit-Domìnguez, M.D., Rucandio, M.I., Gonzàlez, J.A., 2011. Provenance of loess from the Spanish central region: chemometric interpretation. Geological Magazine 148, 481-491.

Giorgi, F., Lionello, P., 2008. Climate change projections for the Mediterranean region. Global and Planetary Change 63, 90-104.

González-Sampériz, P., Leroy, S.A.G., Carrión, J.S., Fernández, S., García-Antón, M., Gil-García, M.J., Uzquiano, P., Valero-Garcés, B., Figueiral, I., 2010. Steppes, savannahs, forests and phytodiversity reservoirs during the Pleistocene in the Iberian Peninsula. Review of Palaeobotany and Palynology 162, 427-457.

González-Sampériz, P., Valero-Garcés, B.L., Moreno, A., Jalut, G., García-Ruiz, J.M., Martí-Bono, C., Delgado-Huertas, A., Navas, A., Otto, T., Dedoubat, J.J., 2006. Climate variability in the Spanish Pyrenees during the last 30,000 yr revealed by the El Portalet sequence. Quaternary Research 66, 38-52.

Gülz, P.-G., 1994. Epicuticular Leaf Waxes in the Evolution of the Plant Kingdom. Journal of Plant Physiology 143, 453-464.

Häggi, C., Zech, R., McIntyre, C., Zech, M., Eglinton, T.I., 2014. On the stratigraphic integrity of leaf-wax biomarkers in loess paleosols. Biogeosciences 11, 2455-2463.

Hoefs, M.J.L., Rijpstra, W.I.C., Sinninghe Damsté, J.S., 2002. The influence of oxic degradation on the sedimentary biomarker record I: evidence from Madeira Abyssal Plain turbidites. Geochimica et Cosmochimica Acta 66, 2719-2735.

Lewis, C.J., McDonald, E.V., Sancho, C., Peña, J.L., Rhodes, E.J., 2009. Climatic implications of correlated Upper Pleistocene glacial and fluvial deposits on the Cinca and Gállego Rivers (NE Spain) based on OSL dating and soil stratigraphy. Global and Planetary Change 67, 141-152.

Maffei, M., Badino, S., Bossi, S., 2004. Chemotaxonomic significance of leaf wax n-alkanes in the Pinales (Coniferales). Journal of Biological Research 1, 3-19.

Mihailova, A., Abbado, D., Pedentchouk, N., 2015. Differences in n-alkane profiles between olives and olive leaves as potential indicators for the assessment of olive

leaf presence in virgin olive oils. European Journal of Lipid Science and Technology 117, 1480-1485.

Moreno, A., González-Sampériz, P., Morellón, M., Valero-Garcés, B.L., Fletcher, W.J., 2012. Northern Iberian abrupt climate change dynamics during the last glacial cycle: A view from lacustrine sediments. Quaternary Science Reviews 36, 139-153.

Moreno, A., Svensson, A., Brooks, S.J., Connor, S., Engels, S., Fletcher, W., Genty, D., Heiri, O., Labuhn, I., Perşoiu, A., Peyron, O., Sadori, L., Valero-Garcés, B., Wulf, S., Zanchetta, G., 2014. A compilation of Western European terrestrial records 60–8 ka BP: towards an understanding of latitudinal climatic gradients. Quaternary Science Reviews 106, 167-185.

Nierop, K.G.J., Verstraten, J.M., 2003. Organic matter formation in sandy subsurface horizons of Dutch coastal dunes in relation to soil acidification. Organic Geochemistry 34, 499-513.

Pallàs, R., Rodés, Á., Braucher, R., Carcaillet, J., Ortuño, M., Bordonau, J., Bourlès, D., Vilaplana, J.M., Masana, E., Santanach, P., 2006. Late Pleistocene and Holocene glaciation in the Pyrenees: a critical review and new evidence from $^{10}$Be exposure ages, south-central Pyrenees. Quaternary Science Reviews 25, 2937-2963.

Pantaléon-Cano, J., Yll, E.-I., Pérez-Obiol, R., Roure, J.M., 2003. Palynological evidence for vegetational history in semi-arid areas of the western Mediterranean (Almería, Spain). The Holocene 13, 109-119.

553 Poynter, J.G., 1989. Molecular stratigraphy: the recognition of palaeoclimatic
554 signals in organic geochemical data. University of Bristol, Bristol.
555 Poynter, J.G., Farrimond, P., Robinson, N., Eglinton, G., 1989. Aeolian-derived
556 higher plant lipids in the marine sedimentary record: links with paleoclimate,
557 Paleoclimatology and Paleometeorology: Modern and Past Patterns of Global
558 Atmospheric Transport. Kluwer Academic, Hingham, Mass, Dordrecht, pp. 435–
559 462.
560 Prentice, I.C., Guiot, J., Harrison, S.P., 1992. Mediterranean vegetation, lake levels
561 and palaeoclimate at the Last Glacial Maximum. Nature 360, 658-660.
562 Rodríguez-Sánchez, F., Hampe, A., Jordano, P., Arroyo, J., 2010. Past tree range
563 dynamics in the Iberian Peninsula inferred through phylogeography and
564 palaeodistribution modelling: A review. Review of Palaeobotany and Palynology
565 162, 507-521.
566 Rommerskirchen, F., Plader, A., Eglinton, G., Chikaraishi, Y., Rullkötter, J., 2006.
567 Chemotaxonomic significance of distribution and stable carbon isotopic
568 composition of long-chain alkanes and alkan-1-ols in $C_4$ grass waxes. Organic
569 Geochemistry 37, 1303-1332.
570 Roquero, E., Silva, P.G., Goy, J.L., Zazo, C., Massana, J., 2015. Soil evolution indices
571 in fluvial terrace chronosequences from central Spain (Tagus and Duero fluvial
572 basins). Quaternary International 376, 101-113.
573 Sachse, D., Billault, I., Bowen, G.J., Chikaraishi, Y., Dawson, T.E., Feakins, S.J.,
574 Freeman, K.H., Magill, C.R., McInerney, F.A., van der Meer, M.T.J., Polissar, P.,
575 Robins, R.J., Sachs, J.P., Schmidt, H.-L., Sessions, A.L., White, J.W.C., West,

576 J.B., Kahmen, A., 2012. Molecular Paleohydrology: Interpreting the Hydrogen-
577 Isotopic Composition of Lipid Biomarkers from Photosynthesizing Organisms.
578 Annual Review of Earth and Planetary Sciences 40, 221-249.
579 Sachse, D., Radke, J., Gleixner, G., 2006. δD values of individual n-alkanes from
580 terrestrial plants along a climatic gradient – Implications for the sedimentary
581 biomarker record. Organic Geochemistry 37, 469-483.
582 Schäfer, I.K., Lanny V., Eglinton, T.I., Zech, M., Zech, R., submitted. The role of
583 vegetation, degradation and climate for leaf waxes in litter and topsoils in
584 Europe.
585 Schwark, L., Zink, K., Lechterbeck, J., 2002. Reconstruction of postglacial to early
586 Holocene vegetation history in terrestrial Central Europe via cuticular lipid
587 biomarkers and pollen records from lake sediments. Geology 30, 463-466.
588 Seager, R., Liu, H., Henderson, N., Simpson, I., Kelley, C., Shaw, T., Kushnir, Y.,
589 Ting, M., 2014. Causes of Increasing Aridification of the Mediterranean Region
590 in Response to Rising Greenhouse Gases. Journal of Climate 27, 4655-4676.
591 Tarasov, P.E., Müller, S., Zech, M., Andreeva, D., Diekmann, B., Leipe, C., 2013.
592 Last glacial vegetation reconstructions in the extreme-continental eastern Asia:
593 Potentials of pollen and n-alkane biomarker analyses. Quaternary International
594 290–291, 253-263.
595 Tipple, B.J., Pagani, M., 2010. A 35 Myr North American leaf-wax compound-
596 specific carbon and hydrogen isotope record: Implications for $C_4$ grasslands and
597 hydrologic cycle dynamics. Earth and Planetary Science Letters 299, 250-262.

598 Tipple, B.J., Pagani, M., 2013. Environmental control on eastern broadleaf forest
599 species' leaf wax distributions and D/H ratios. Geochimica et Cosmochimica Acta
600 111, 64-77.
601 Vogts, A., Schefuß, E., Badewien, T., Rullkötter, J., 2012. *n*-Alkane parameters from
602 a deep sea sediment transect off southwest Africa reflect continental vegetation
603 and climate conditions. Organic Geochemistry 47, 109-119.
604 Wang, N., Zong, Y., Brodie, C.R., Zheng, Z., 2014. An examination of the fidelity of
605 *n*-alkanes as a palaeoclimate proxy from sediments of Palaeolake Tianyang,
606 South China. Quaternary International 333, 100-109.
607 Wolf, D., Faust, D. (2015): Western Mediterranean environmental changes:
608 Evidences from fluvial archives. Quaternary Science Reviews
609 (QSR) 122, 30 – 50
610 Zech, M., Andreev, A., Zech, R., Müller, S., Hambach, U., Frechen, M., Zech, W.,
611 2010. Quaternary vegetation changes derived from a loess-like permafrost
612 palaeosol sequence in northeast Siberia using alkane biomarker and pollen
613 analyses. Boreas 39, 540-550.
614 Zech, M., Buggle, B., Leiber, K., Marković, S., Glaser, B., Hambach, U., Huwe, B.,
615 Stevens, T., Sümegi, P., Wiesenberg, G., Zöller, L., 2009. Reconstructing
616 Quaternary vegetation history in the Carpathian Basin, SE-Europe, using *n*-
617 alkane biomarkers as molecular fossils: Problems and possible solutions,
618 potential and limitations. Eiszeitalter und Gegewart. Quaternary Science
619 Journal 58, 148-155.

Zech, M., Rass, S., Buggle, B., Löscher, M., Zöller, L., 2012. Reconstruction of the late Quaternary paleoenvironments of the Nussloch loess paleosol sequence, Germany, using *n*-alkane biomarkers. Quaternary Research 78, 226-235.

Zech, M., Zech, R., Buggle, B., Zöller, L., 2011. Novel methodological approaches in loess research–interrogating biomarkers and compound-specific stable isotopes. Eiszeitalter & Gegenwart-Quatern Sci J 60, 170-187.

Zech, R., Zech, M., Marković, S., Hambach, U., Huang, Y., 2013. Humid glacials, arid interglacials? Critical thoughts on pedogenesis and paleoclimate based on multi-proxy analyses of the loess–paleosol sequence Crvenka, Northern Serbia. Palaeogeography, Palaeoclimatology, Palaeoecology 387, 165-175.

Zhang, Z., Zhao, M., Eglinton, G., Lu, H., Huang, C.-Y., 2006. Leaf wax lipids as paleovegetational and paleoenvironmental proxies for the Chinese Loess Plateau over the last 170 kyr. Quaternary Science Reviews 25, 575-594.

Zocatelli, R., Lavrieux, M., Disnar, J.-R., Le Milbeau, C., Jacob, J., Bréheret, J., 2012. Free fatty acids in Lake Aydat catchment soils (French Massif Central): sources, distributions and potential use as sediment biomarkers. Journal Soils Sediments 12, 734-748.

## Captions

Fig 1: (a) Map of the sample location, (b) photograph of the research area and (c) the LPS El Paraíso

Fig. 2: Endmember plot modified after Zech et al. (2013) and Schäfer et al. (submitted) with a) plant samples from Central Spain, and b) samples form the LPS El Paraíso. Degradation line grass: 0.129*log(OEP) + 0.5745, degradation line deciduous forests: -0.171*log(OEP) + 0.7459.

Fig. 3: *n*-Alkane proxies in the LPS El Paraíso. From left to right: concentrations of long-chain *n*-alkanes from *n*-$C_{25}$ to *n*-$C_{35}$, OEP, *n*-alkane ratio (*n*-$C_{31}$+*n*-$C_{33}$)/(*n*-$C_{27}$+*n*-$C_{31}$+*n*-$C_{33}$) and grass contribution (%). Loess units are shaded in yellow.

Fig. 4: Ternary plot for *n*-alkanoic acid indices C, D and G with a) plant samples from Central Spain, and b) samples from the LPS El Paraíso. Endmembers for conifers (con), deciduous trees (dec) and grasses (grass) from Central Europe after Schäfer et al. (submitted)

Fig. 5: *n*-Alkanoic acid proxies in the LPS El Paraíso. From left to right: Concentrations of long-chain *n*-alkanoic acids ($C_{20}$-$C_{34}$), EOP, indices C, D and G. Loess units are shaded in yellow.

**Figure 1**

Click here to download high resolution image

**Figure 2**

Click here to download high resolution image

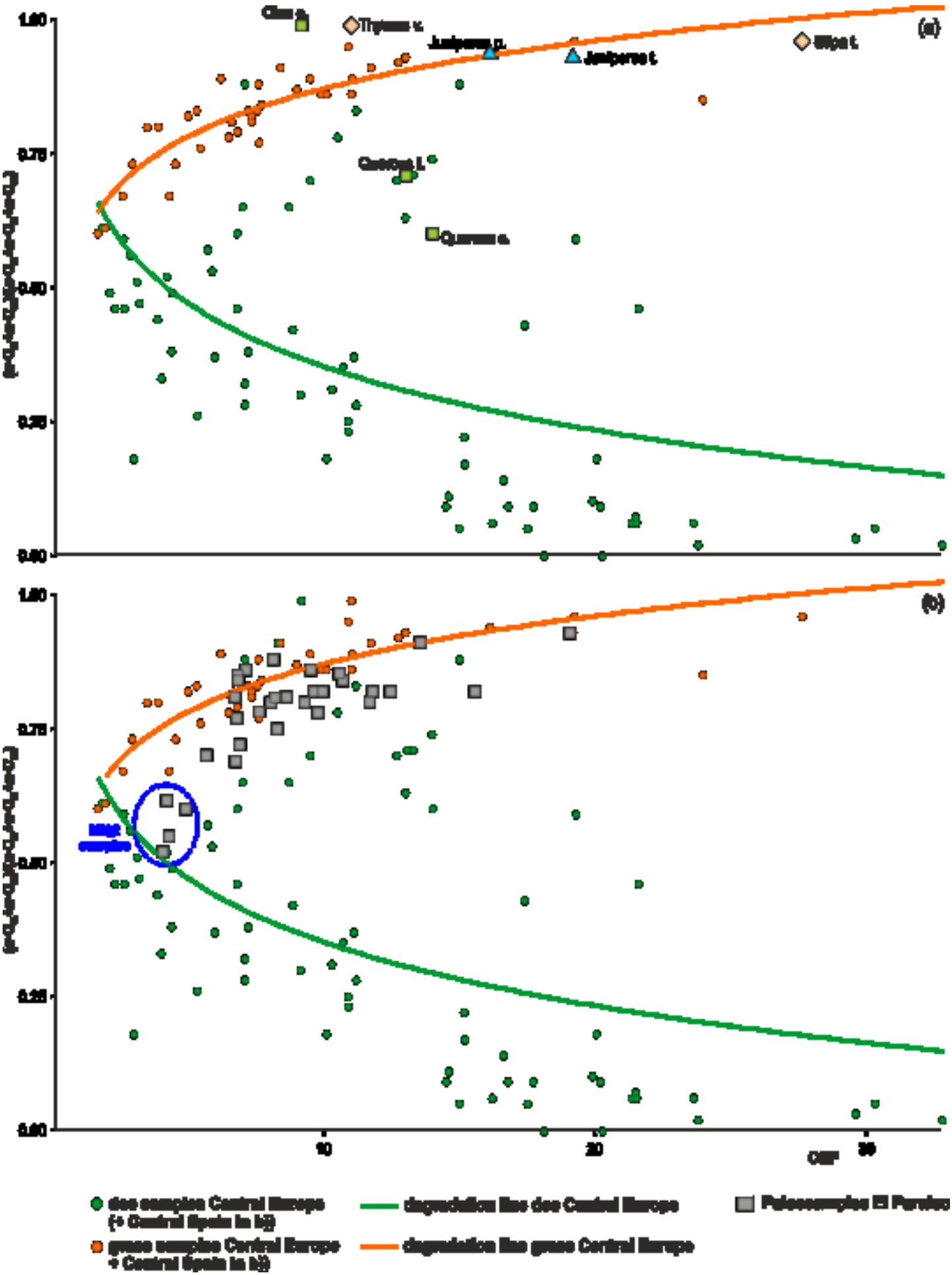

Figure 3

Click here to download high resolution image

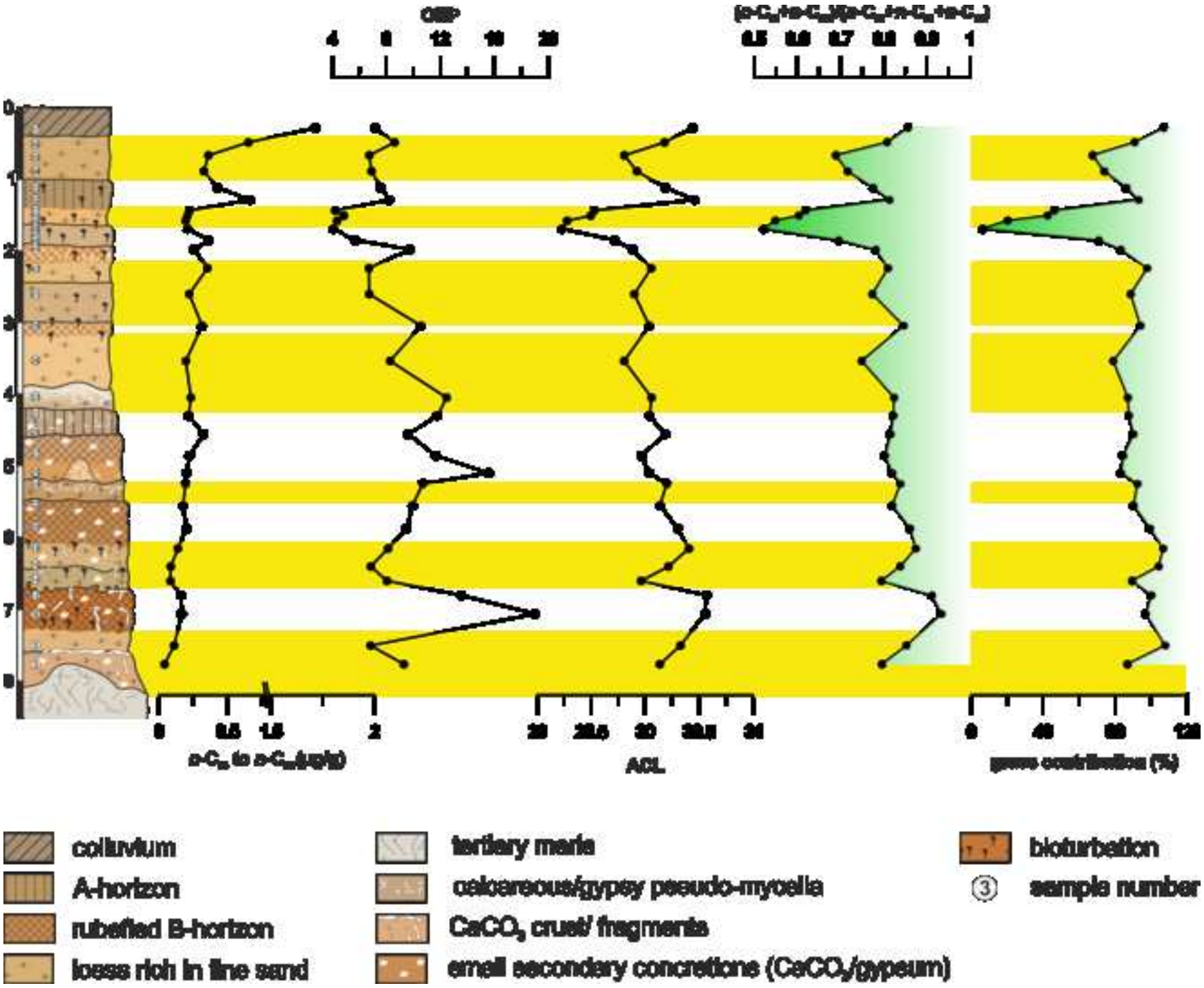

Figure 4

Click here to download high resolution image

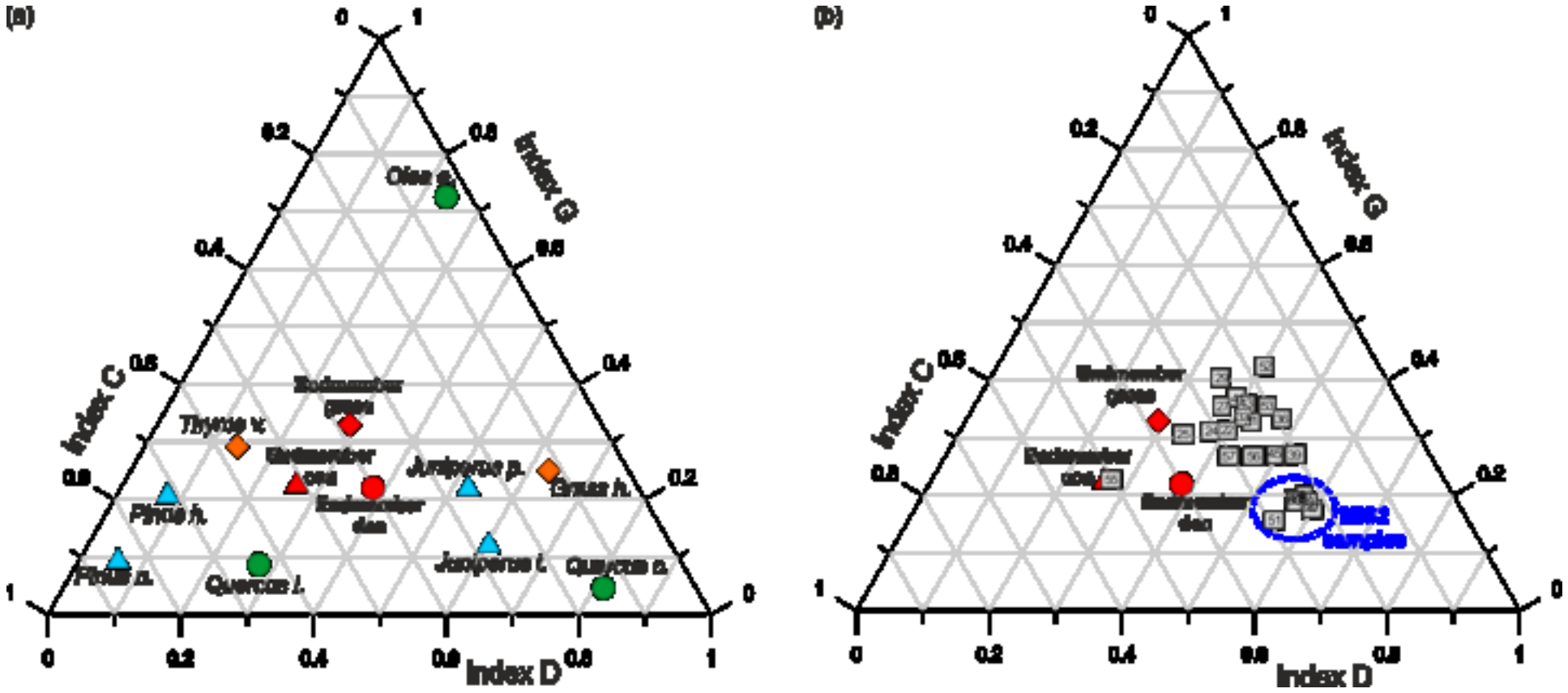

Figure 5

Click here to download high resolution image

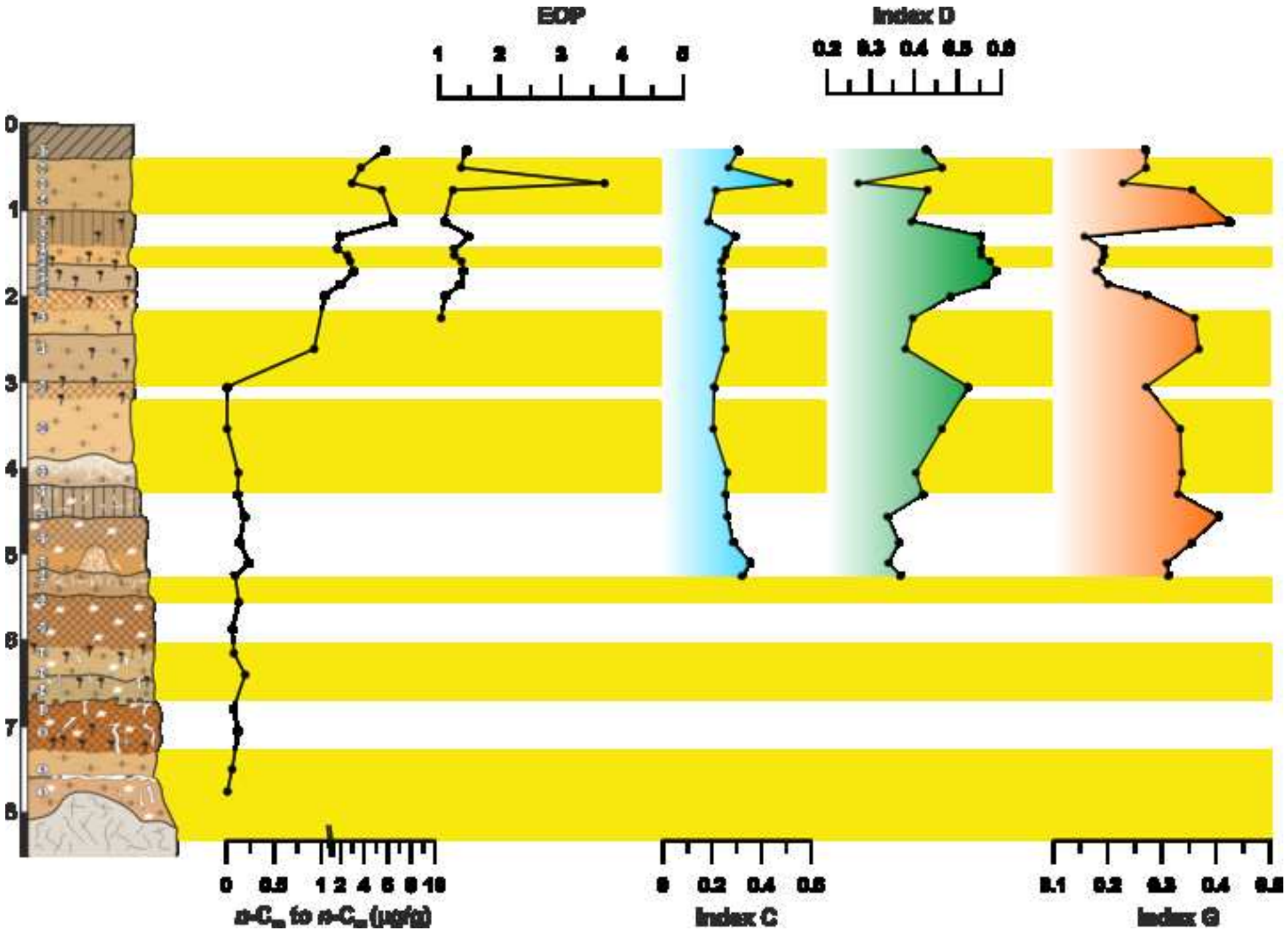

**Table**

Table 1: *n*-alkane distribution in fresh plant material typical for the local vegetation at our sample location

| sample | *n*-$C_{25}$ | *n*-$C_{27}$ | *n*-$C_{29}$ | *n*-$C_{31}$ | *n*-$C_{33}$ | *n*-$C_{35}$ | $c_{tot}$ | OEP | ACL | (*n*-$C_{31}$+*n*-$C_{33}$)/(*n*-$C_{27}$+*n*-$C_{31}$+*n*-$C_{33}$) |
|---|---|---|---|---|---|---|---|---|---|---|
| *Juniperus phonicea* | 0.42 | 3.55 | 1.88 | 5.60 | 50.13 | 17.29 | 86.11 | 16.13 | 32.35 | 0.94 |
| *Juniperus thurifera* | 0.66 | 3.95 | 3.50 | 12.09 | 80.13 | 13.37 | 121.89 | 19.17 | 32.38 | 0.96 |
| *Pinus nigra* | 0.35 | 0.38 | 0.44 | 0.45 | 3.32 | 0.41 | 6.81 | 4.29 | 31.93 | 0.91 |
| *Pinus halepensis* | 0.35 | 0.42 | 0.43 | 0.42 | 0.37 | 0.40 | 3.87 | 1.52 | 29.90 | 0.65 |
| *Quercus coccifera* | 3.14 | 26.67 | 52.41 | 38.84 | 1.51 | 0.45 | 131.97 | 14.02 | 29.25 | 0.60 |
| *Quercus ilex* | 0.71 | 7.44 | 63.76 | 17.17 | 0.82 | 0.42 | 97.55 | 13.07 | 29.25 | 0.71 |
| *Olea europaea* | 0.28 | 0.86 | 11.05 | 37.89 | 44.85 | 17.10 | 127.73 | 9.15 | 31.68 | 0.99 |
| *Thymus vulgaris* | 1.20 | 2.09 | 39.79 | 125.70 | 175.01 | 8.50 | 390.76 | 11.03 | 31.77 | 0.99 |
| *Stipa tenacissima* | 2.76 | 8.54 | 43.13 | 168.07 | 60.16 | 1.84 | 295.20 | 27.63 | 31.00 | 0.96 |

**Table**

Table 2: *n*-alkanoic acid distribution in the fresh plant material from vegetation typical at our sampling location

| | **Concentration in µg/g sample** | | | | | | | | | | |
|---|---|---|---|---|---|---|---|---|---|---|---|
| **sample** | ***n*-$C_{24}$** | ***n*-$C_{26}$** | ***n*-$C_{28}$** | ***n*-$C_{30}$** | ***n*-$C_{32}$** | ***n*-$C_{34}$** | **Ctot** | **EOP** | **Index C** | **Index D** | **Index G** |
| *Juniperus phonicea* | 1.75 | 1.05 | 3.53 | 1.17 | 0.46 | 1.06 | 12.58 | 5.78 | 0.25 | 0.52 | 0.22 |
| *Juniperus thurifera* | 2.10 | 1.12 | 4.14 | 1.29 | 0.42 | 0.45 | 15.14 | 7.76 | 0.26 | 0.58 | 0.12 |
| *Pinus nigra* | 4.03 | 0.49 | 0.28 | 0.19 | 0.14 | 0.35 | 16.28 | 3.56 | 0.87 | 0.06 | 0.10 |
| *Pinus halepensis* | 5.06 | 0.72 | 0.56 | 0.67 | 0.56 | 1.02 | 32.38 | 5.00 | 0.74 | 0.08 | 0.22 |
| *Quercus coccifera* | 3.78 | 13.40 | 16.32 | 7.50 | 0.86 | 0.07 | 62.49 | 11.06 | 0.13 | 0.78 | 0.04 |
| *Quercus ilex* | 5.81 | 1.23 | 1.53 | 5.00 | 0.45 | 0.03 | 25.39 | 11.75 | 0.45 | 0.20 | 0.06 |
| *Olea europaea* | 0.85 | 1.56 | 4.80 | 8.10 | 9.64 | 5.03 | 35.80 | 8.25 | 0.04 | 0.24 | 0.72 |
| *Thymus vulgaris* | 8.95 | 6.61 | 1.92 | 4.10 | 2.06 | 1.97 | 37.91 | 10.47 | 0.53 | 0.13 | 0.27 |
| *Stipa tenacissima* | 1.21 | 2.30 | 4.74 | 3.02 | 1.59 | 0.30 | 17.76 | 11.29 | 0.11 | 0.60 | 0.24 |

*Detailed Response to Reviewers

UNIVERSITÄT BERN
OESCHGER CENTRE
CLIMATE CHANGE RESEARCH

Imke Kathrin Schäfer
Institute of Geography
University of Bern
Hallerstrasse 12
CH- 3012 Bern
+41(0) 31 631 8890
imke.schaefer@giub.unibe.ch

Dear editors of Quaternary International,

Please find attached the revised version of our manuscript entitled

Evidence for humid conditions during the last glacial from leaf wax patterns in the loess-paleosol sequence El Paraíso, Central Spain

by Imke K. Schäfer, Marcel Bliedtner, Daniel Wolf, Dominik Faust, Roland Zech

We thank the anonymous reviewer for his comments and suggestions. We revised our manuscript accordingly:

1: The English for our manuscript was corrected by a native speaker (service from the Oeschger Centre for Climate Change Research)
2: We deleted Lines 231-233 as suggested. We prefer, however, to keep lines 399-405. Those give an outlook for our ongoing work.
3: Lines 290-293: To our knowledge there are no published pollen record that support a humid LGM, which we clarified in the revised manuscript.
4: Lines 356-361: We agree with the reviewer that an arid climate and hence a low vegetation density can be an additional explanation for the low *n*-alkanoic acid concentrations. We now included this in the discussion.
5: As suggested by the reviewer we modified the discussion concerning the agreement of our results with previous findings. This now reads as: Our results and interpretation are in line with fluvial and lacustrine records from Iberia, which suggest there were more humid conditions during the global LGM, probably due to a southward shift of the westerlies and storm tracks (Moreno et al., 2012; Moreno et al., 2014; Beghin et al., 2015). Our results and interpretation are also in line with genetic features of recent European tree populations, which show that tree species survived in glacial refugia in Southern Europe during the last glacial (Carrión et al., 2003; González-Sampériz et al., 2010).
6: We replaced “Conclusion” with “Conclusions” as the reviewer requested

With many thanks for your efforts

Yours sincerely,

Imke Schäfer